A Fractional-Order Model of the Cardiac Function

Guel-Cortez, A-J. & Kim, E.

Original citation:
'A Fractional-Order Model of the Cardiac Function', in Chaotic Modeling and Simulation International Conference, ed. by Christos H. Skiadas, Yiannis Dimotikalis pub 2021 (ISBN 978-3-030-70794-1)

Publisher: Springer

A fractional-order model of the cardiac function (PREPRINTver)

Adrian-Josue Guel-Cortez   Eun-jin Kim

December 20, 2021

Abstract

Improving the mathematical model of the cardiovascular system is an important aspect of the control and design of ventricular assist devices. In this work, through numerical simulations, we analyse the usage of fractional-order operators as a way to improve the circulation model. More specifically, we show that the use of fractional-order derivatives in the lumped circulation model can create different types of heart anomalous behaviours. This includes aortic regurgitation, mitral stenosis and ischaemic cardiomyopathy.

1 Introduction

In 2015, 17.9 million people died around the world caused by cardiovascular disease and rose by 12.5% between 2005 and 2015 with a specific increase of ischaemic heart disease by 16.6% [1]. Even though heart transplantation is considered as the best therapy for patients with end-stage congestive heart failure [2], it is usually a delayed process that could last around 300 days or more on the average for potential recipients. For this reason, the medical community has increased emphasis on the use of ventricular assist devices (VADs) that can enhance the function of the natural heart while patients wait for heart transplantation. These ventricular assists devices are mechanical devices that help the heart with the pumping of the blood through the circulatory system (left ventricular assists device (LVAD)) or through the pulmonary system (right ventricular assist device (RVAD)) [3, 4, 5]. There are currently different types of VADs [6, 7], but the usual consists of a rotary pump applied to the left ventricle [6].

To design proper VADs, different mathematical models for the cardiovascular system have been considered (for instance, see [8, 9]). These are categorised as zero-dimensional (0-D) or lumped parameter models and distributed parameter models or 1-D, 2-D and 3-D models [10]. The mathematical model must be able to properly characterise the cardiac cycle but also important aspects like heart failure (usually studied by pressure-volume (PV) loop analysis [11]), which is a relevant element in VADs' control design [12, 13]. Besides, even though higher dimension models may better describe the heart dynamics, we have to consider that it is a challenge to analyse control strategies for VADs when using such models [3]. Therefore, we require a mathematical model that could represent the heart complex dynamics while being as simple as possible.

An elementary way to describe the heart dynamics (including VADs) is by the use of Windkessel models which are represented through electrical or mechanical networks [14, 3]. Nonetheless, such simplicity has its drawbacks, for instance, the basic two-element Windkessel model explains aortic pressure decay in diastole, but it fails shortly in systole [10]. A way to overcome such drawback consists of adding more elements to the electrical representation [15, 16, 17]. Recently. in [18] a different approach has been proposed to solve this problem, it consists in the use of fractional-order operators (derivatives or integrals of non-integer order [19]) in the arterial Windkessel model. When talking about fractional-order operators, heterogeneous systems and phenomena exhibiting anomalous diffusion can be well fitted by using fractional-order derivatives [20, 21]. Examples of such systems are biological tissues [22] and large-scale complex networks [23, 24]. It is important to mention that fractional-order operators does not complicate control design, since there are numerous approaches for control of fractional-order systems that can be implemented (for instance, see [25]). This implies that fractional order operators, when added to the cardiovascular model are a feasible option that may better describe a wider range of real-case scenarios.

Considering the previous lines, in this work, we provide a qualitative analysis of the use of fractional-order operators in the lumped circulatory model by considering two different mathematical models from the literature. This analysis demonstrates that fractional-operators extend the capabilities of such models in the PV loop analysis. Specifically, we add fractional-order operators to modify the rate of change of the aortic, atrial and arterial pressures in the circulation model. These changes permit us to create different anomalous behaviours in the PV loops that resemble aortic regurgitation, mitral stenosis or ischaemic cardiomyopathy dynamics. The remainder of this paper is organised as follows: Section 2 presents the basic concepts and their connection with this work. In Section 3, our main results are provided. Finally, Section 4 contains our concluding remarks.

2 Preliminary results

In the following subsections, we offer a description of the background knowledge that will be useful to the reminder of this work.

2.1 The mathematical model

We base our analysis by considering the mathematical models of the cardiovascular system with LVAD presented in [5] and [4].

Firstly, in [4], a fifth-order lumped parameter electric circuit to reproduce the left ventricle hemodynamics of the heart is used. This model assumes that the right ventricle and pulmonary circulation are healthy and normal. Also, a simple first-order forced differential equation to represent the LVAD is considered (see Figure 1). Furthermore, [4] uses a time-varying capacitance (compliance), which is derived by system identification procedures, to describe the contractual state of the left ventricle. On the other hand, [5, 26] presents a mathematical model of the cardiac function that integrates mechanical, electric and chemical activity on micro-scale sarcomere and macro-scale heart. More specifically, this model includes the fifth-order lumped parameter electric circuit as well as the electrical model for the LVAD from [4] but presents a different mathematical model of the mechanical, electric and chemical activity to describe the behaviour of the contractual state in the left ventricle.

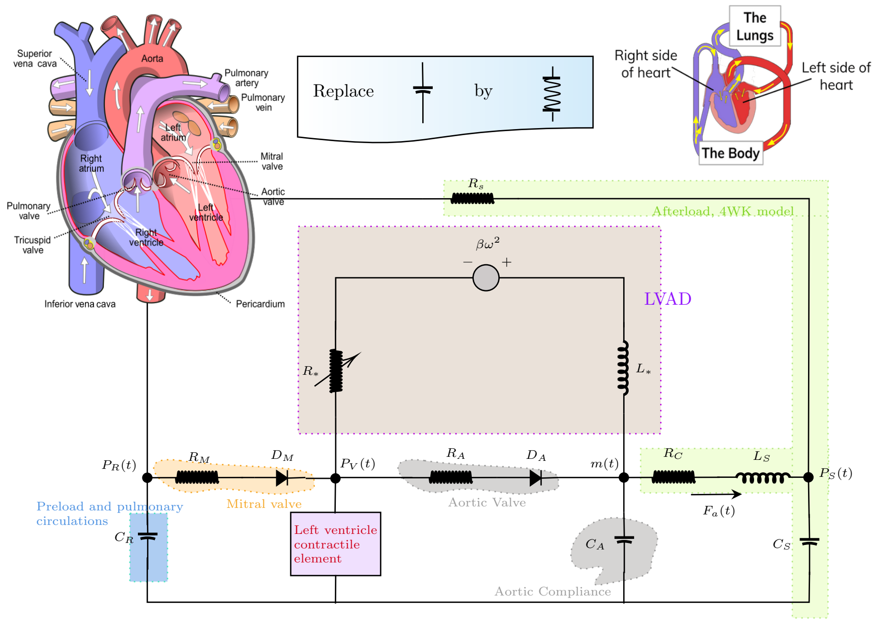

Figure 1: Lumped parameter electric circuit used to reproduce the left ventricle hemodynamics of the heart and LVAD.

Recalling from [5], the governing equations of the electric circuit shown in Figure 1 are given by

$$\begin{aligned}
\frac{dV}{dt} &= \frac{1}{R_m}(P_R - P_V)\,\Theta(P_R - P_V) - \frac{1}{R_A}(P_V - m)\,\Theta(P_V - m) - \delta_p n, \\
\frac{dm}{dt} &= -\frac{1}{C_A}F_a + \frac{1}{C_A R_A}(P_V - m)\,\Theta(P_V - m) + \delta_p \frac{n}{C_A}, \\
\frac{dF_a}{dt} &= \frac{m - P_S}{L_S} - \frac{R_C F_a}{L_S}, \\
\frac{dP_R}{dt} &= \frac{-P_R + P_S}{C_R R_S} - \frac{1}{C_R R_M}(P_R - P_V)\,\Theta(P_R - P_V), \\
\frac{dP_S}{dt} &= \frac{P_R - P_S}{C_S R_S} + \frac{F_a}{C_S}.
\end{aligned} \tag{1}$$

Where V stands for the left ventricular volume, m is the aortic pressure, n corresponds to the pump flow, F_a is the aortic total flow, P_R stands for the atrial pressure and P_S is the arterial pressure. Besides, the function $\Theta(u)$ is a Heaviside function which takes the non-zero value of 1 for $u > 0$ or 0 otherwise. Moreover, the equation governing the pump flow is

$$\frac{dn}{dt} = \frac{1}{L_*}\left[P_V - m - R_* n + \beta\omega^2\right]. \tag{2}$$

In this work, we will consider no pump support. This can be set up by using $\delta_p = 0$. In addition, we use the same set of parameter values presented in [4] for its model and the same set for [5]'s model when considering a case that shows ectopic PV loop oscillations using $\mu_1 = 0.0024$ and $\mu_2 = 0.1584$ on its electric activity model.

2.1.1 Fractional-order Windkessel model

As we have mentioned in Section 1, the goal of this work is to study the addition of fractional order operators in the lumped parameter circulation model (1). Recently, [27, 18] proposes a fractional-order Windkessel model as an alternative to improve the systolic phase model description. Inspired on the same approach, in Figure 2a, we introduce a two-element Windkessel model that uses a fractance element C_F^α. This fractance element is equivalent to an infinite tree of capacitors and resistors [28]. When this infinite tree is binary, it is proved to be of order $\alpha = \frac{1}{2}$ (for further details, see [29, 23, 24]). To change α's value, we can use the procedure described in [30] which consists of allowing more complicated fractal networks or recursive trees to be constructed (see Fig. 2b). Hence, using a fractional-order capacitor is equivalent to adding a fractal network in the circuit.

For a better understanding of the mathematical description behind a fractional-order capacitor, consider the model for the fractional-order circuit shown in Fig. 2a. This model is given by

$$ {}_0\mathcal{D}_t^\alpha P_a = \frac{Q_a}{C_F^\alpha} - \frac{P_a}{RC_F^\alpha}. \tag{3}$$

Taking in to account expression (3). We have the following result

Proposition 1 *By using the Caputo definition of the fractional derivative operator ${}_0\mathcal{D}_t^\alpha$ of order $0 < \alpha < 1$ [31]. The time response of system* (3) *is given by*

$$ P_a(t) = P_a(0)t^{\alpha-1}\mathbf{E}_{\alpha,\alpha}\left(-\frac{1}{RC_F^\alpha}t^\alpha\right) + \frac{1}{C_F^\alpha}\int_0^t Q_a(t-\tau)\tau^{\alpha-1}\mathbf{E}_{\alpha,\alpha}\left(-\frac{1}{RC_F^\alpha}\tau^\alpha\right)d\tau, \tag{4}$$

where $\mathbf{E}_{\alpha,\alpha}(z)$ is the Mittag-Leffler function of the complex value z [32].

Proof 1 *The proof follows by applying the Laplace transform to* (3) *and obtain the inverse Laplace transform $\mathscr{L}^{-1}[P_a(s)]$.*

An important conclusion from Proposition 1 is that equation (4) describes the arterial pressure as a power low equation with a diffusive term. This kind of representation implies some challenges that have been recently discussed through various works (for instance, see [33, 34] and the references therein). Taking the previous lines into consideration, it is important to mention that instead of finding an analytical solution to our set of differential equations, in this work, we will offer a qualitative analysis by numerically solving our set of fractional order differential equations. The numerical solution will be computed by using the methods presented in [35], which consider that the fractional derivative of order $0 < \alpha \leq 1$ of a continuously differentiable real-valued function $x(t)$ is found by taking $x(t) = 0$ for all $t < 0$.

2.2 Pressure–volume loop analysis in cardiology

Since our analysis will focus on the behaviours obtained using fractional-order derivatives in left ventricular PV loops, it is important to define why PV loops are a critical feature to study. We can describe PV loop analysis as a reference method that offers unique insights into mechanical cardiac efficiency. This includes the understanding of the pathophysiology, diagnosis, and treatment of myocardial ischaemia, mitral and aortic regurgitation, mitral and aortic stenosis, and others (for further details, see [36, 37]).

In summary, as shown in Figure 3, a PV loop plots the changes in ventricular pressure associated with the changes in volume occurring during a cardiac cycle. A full description of the different

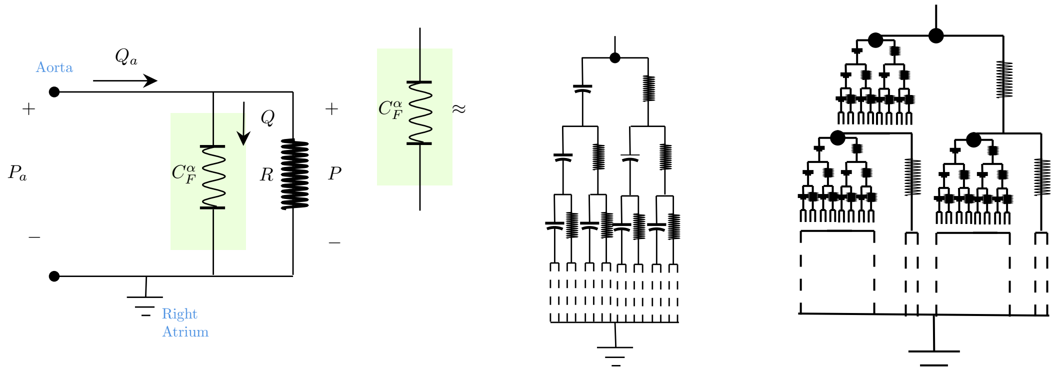

a Fractional-order Windkessel model. b Recursive fractal tree model.

Figure 2: Diastole and Systole response of the two element WK model.

concepts related to volumes, pressures, and areas in a PV loop (shown in Figure 3) can be found in [38]. Below, we describe some of the pressure-volume concepts that will be of main interest in this work

- The end-diastolic pressure volume relationship (EDPVR) (black dashed line). The slope of this line gives the elastance of the ventricle. An important value over this line corresponds to the End-diastolic volume (EDV) or preload, which helps to determine the initial value of the arterial elastance line (shown as a red dashed line in Figure 3).
- The stroke volume. This is the difference between the end-diastolic volume and the end-systolic volume. It is also known as the ejection fraction, i.e. the amount of blood to be ejected by the left ventricle to the circulatory system.
- Arterial elastance line (red dashed line). This line allow us to measure the afterload which is technically given by the pressure-volume relationship throughout the entire of ejection, but assumed to be the slope of such a line drawn from the x-axis value of EDV to the end systolic pressure value in point A.
- The slope of the End-systolic pressure volume-relationship (ESPVR) also known as contractility (blue dashed line). It also represents the elastance at end-systole E_{es}.
- The stroke work, which corresponds to the green shaded area of the PV loop.
- The four stages in the PV loop given by: **A**-Aortic valve closing, **B**-Mitral valve opening, **C**-Mitral valve closing and **D**-Aortic valve opening.

3 Main results

In this section, we present the main results of our analysis. We start by describing how we modify equations (1) to include fractional-order dynamics. Then, we vary the fractional-order derivative orders and comment on their individual and grouped effects. Finally, we simulate the behaviour of the fractional-order circulation model when changing other parameters in the circuit.

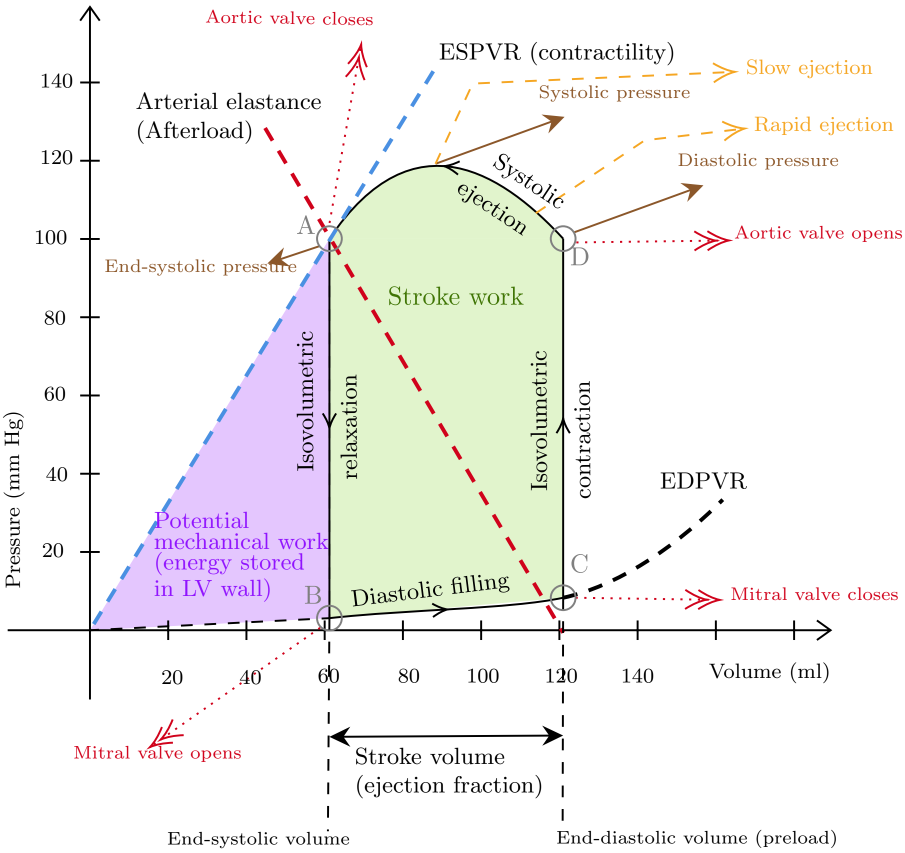

Figure 3: PV loop diagram.

3.1 The fractional-order circulation model

Consider the use of fractances in the left atrial, aortic and systemic compliances of the lumped parameter electric circuit shown in Figure 1. Thus, equations for the left atrial pressure P_R, the aortic pressure m and the arterial pressure P_S in (1) are rewritten as

$$\begin{aligned} \frac{d^{\alpha_m} m}{dt^{\alpha_m}} &= -\frac{1}{C_A} F_a + \frac{1}{C_A R_A} (P_V - m)\, \Theta\,(P_V - m) + \delta_p \frac{n}{C_A}, \\ \frac{d^{\alpha_R} P_R}{dt^{\alpha_R}} &= \frac{-P_R + P_S}{C_R R_S} - \frac{1}{C_R R_M} (P_R - P_V)\, \Theta\,(P_R - P_V)\,, \\ \frac{d^{\alpha_S} P_S}{dt^{\alpha_S}} &= \frac{P_R - P_S}{C_S R_S} + \frac{F_a}{C_S}. \end{aligned} \tag{5}$$

where $\alpha_m, \alpha_R, \alpha_S \in (0, 1]$ are the fractional orders of the time derivatives for m, P_R and P_S, respectively.

3.2 The role of α_S

To understand the role of α_m, α_R and α_S in the circulation model, we linearly vary these parameters in [4]'s and [5]'s models. First, we analyse the effect of α_S. If we let $\alpha_m, \alpha_R = 1$ and only vary $\alpha_S \in (0, 1]$, in mathematical terms, we are adding an infinite memory and non-local operator to describe the rate of the arterial-pressure. Physically speaking, since the capacitor for the arterial compliance in the circuit tries to model the biggest part of the cardiovascular system, when adding a fractance (an infinite network of resistors and capacitors), we are trying to improve the description of the arterial system by implicitly adding an infinite number of elements.

Figures 4a and 4b show the process of decreasing α_S from 1 to 0.2. This process scarcely changes the stroke work but creates an attractor that shows a right-shift of the PV loop in both model's responses (with a greater factor in [5]'s model). Such a shift to the right is presented in ischaemic cardiomyopathy [37]. Besides, the slope of the ESPVR remains almost the same and the afterload slope shows small increments.

Moreover, a specific analysis in [5]'s model (Fig. 4b) shows that PV loops with ectopic behaviours using $\alpha_m = \alpha_R = \alpha_S = 1$ completely change when $\alpha_S < 0.6$. This change shows a little increase in afterload and EDV which is quite similar to the one presented in aortic regurgitation. Finally, when $\alpha < 0.3$, the PV loop shows a progressive right-shifting greater than in [4]'s model.

3.3 The role of α_R

The value of α_R and α_m mathematically and physically contain the same properties than α_S, but their role in the circulation model is different. If we consider α_R, this affects the rate of change in the atrial pressure. Here, Figure 5 presents the simulations when changing α_R in the models of [5] and [4] while fixing $\alpha_m = \alpha_S = 1$. First, from Figure 5a, we can see that for $\alpha_R < 1$ there is a gradual right-shift of the PV as in the case of α_S, but there is also a monotonically increasing preload that is a characteristic feature of aortic regurgitation. Analysing Figure 5b, [5]'s model initially presented an anomalous behaviour using $\alpha_R = \alpha_m = \alpha_S = 1$ which is normalised when $\alpha_R < 0.7$ while showing a behaviour similar to the case of [4]'s model but in small proportions.

3.4 The role of α_m

Since the aorta is the main artery that carries blood away from the heart to the rest of the body, aortic pressure plays an imperative role in the cardiovascular system. Also, the aortic pressure is

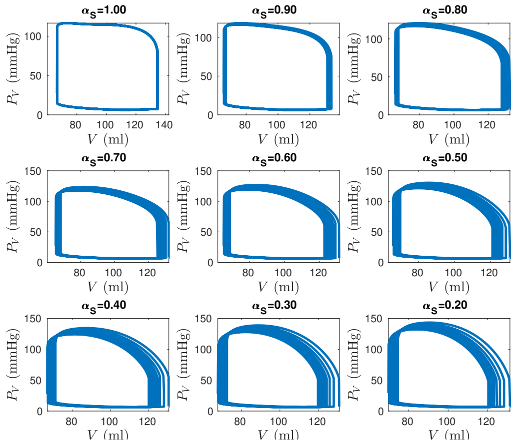

a Changes using [4]'s model.

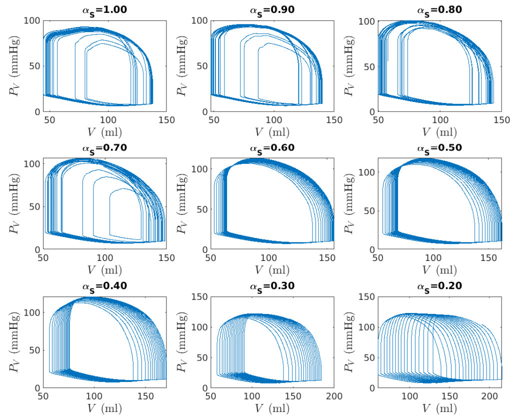

b Changes using [5]'s model.

Figure 4: Changes in α_S with $\alpha_m = \alpha_R = 1$ using the models of [5] and [4].

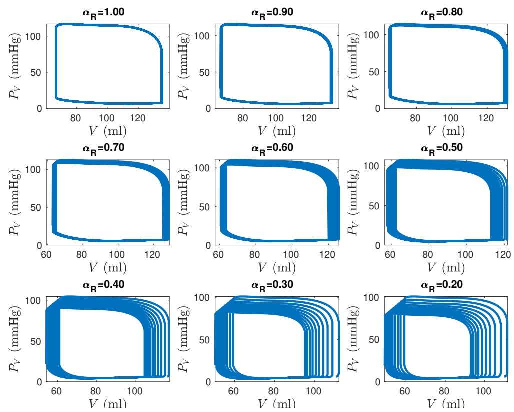

a Changes using [4]'s model.

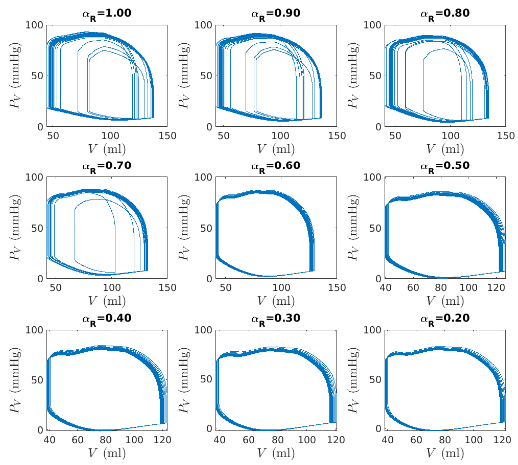

b Changes using [5]'s model.

Figure 5: Changes in α_R with $\alpha_m = \alpha_S = 1$ using the models of [5] and [4].

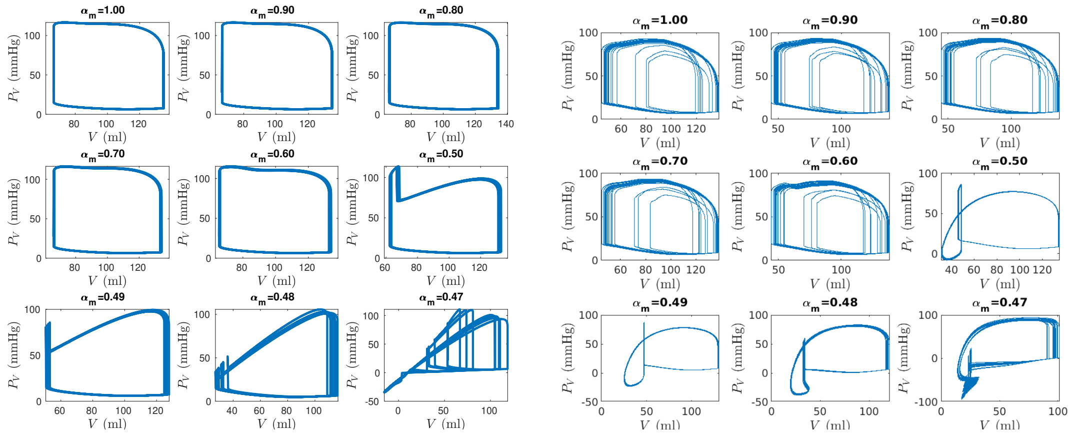

a Changes using [4]'s model. b Changes using [5]'s model.

Figure 6: Changes in α_m with $\alpha_R = \alpha_S = 1$ using the models of [5] and [4].

affected by the ventricular pressure whose behaviour is modified by using different mechanic-electric models (to describe the ventricular contraction) or by the mitral valve functioning. In this context, the value of α_m plays a crucial role, because it directly affects the rate of change in the aortic pressure.

Here, we perform simulations of both [5] and [4] models when changing α_m and fixing $\alpha_R = \alpha_S = 1$. For both models, we have an erratic PV behaviour that includes negative diastolic pressures when $\alpha_m < 0.6$. The presence of negative diastolic pressure values is a phenomenon that has been studied since long ago as an effect of mitral stenosis [39]. Nonetheless, since the simulation stops working when $\alpha_m < 0.47$, this erratic performance seems to be caused by numerical errors in both models. Such numerical inconsistencies may be fixed by using a smaller integration step but paying a high computational cost.

3.5 Changing fractional-orders equally and the effect of other parameters

As we have seen from previous sections, changing α_m, α_R and α_S separately while fixing the other parameters give an insight about their effect on the cardiovascular model. Here, in Figure 7, we show the influence of adding equal and unequal fractional-order values. Such simulations show the presence of a slight right-shifting over time but with no highly anomalous behaviours. In this case, the use of fractional-order operators seems to transform the PV loop into a quasi-periodic attractor for [4]'s model and erase the ectopic oscillations while increasing the stroke volume for [5]'s model.

Finally, some of the parameters in the circulation model (1) are known to produce certain effects. For example, the value of R_m decrease/increase the stroke volume by changing the ESV and EDV positions while fixing ESPVR and changing R_S decrease/increase the stroke volume by fixing ESPVR but changing the afterload. Since this effect has been studied using [4]'s model, Figure 8 only shows the effects of R_m and R_S on this model while using fixed $\alpha_m = \alpha_R = \alpha_S = 0.7$. These simulations show that the effects of R_m and R_S prevail while the fractional-order derivatives continue adding a right-shifting.

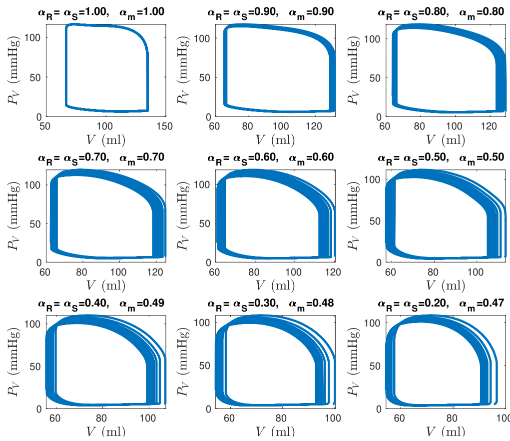

a Changes using [4]'s model.

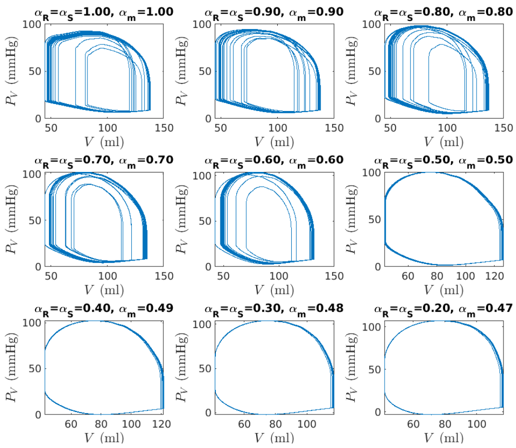

b Changes using [5]'s model.

Figure 7: Changes in $\alpha_m, \alpha_R, \alpha_S$ using the models of [4] and [5].

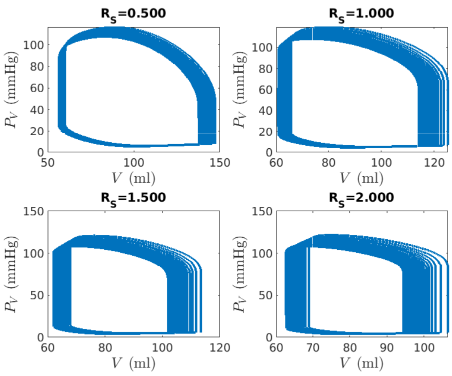

a Changes in R_S.

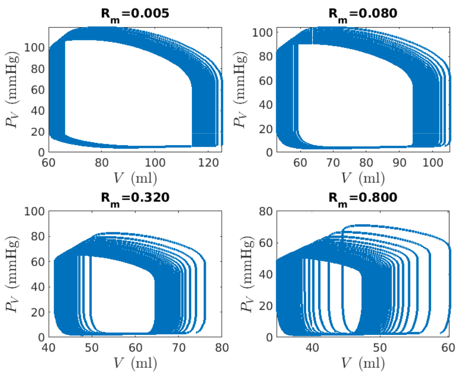

b Changes in R_m.

Figure 8: Changes in R_S and R_m with $\alpha_m = \alpha_R = \alpha_S = 0.7$ using [4]'s model.

4 Concluding remarks

In this work, we have introduced a qualitative analysis of the use of fractional-order operators in two cardiovascular models with distinct left ventricular contractile element models, by adding fractances instead of capacitors to represent aortic, atrial and arterial compliances. Moreover, through PV loop analysis, we have demonstrated that fractional-order derivatives can help to characterise heart anomalous behaviours. Specifically, it may help at describing aortic regurgitation, mitral stenosis and ischaemic cardiomyopathy. Future work includes the design of a parameter identification technique to fit the parameter's using real data, the inclusion of the LVAD model in the analysis and a controller's design methodology for the LVAD that considers the use of fractional-order derivatives in the model.

References

[1] GBD 2015 Mortality and Causes of Death Collaborators. Global, regional, and national life expectancy, all-cause mortality, and cause-specific mortality for 249 causes of death, 1980-2015: a systematic analysis for the global burden of disease study 2015. *Lancet (London, England)*, 388(10053):1459–1544, 2016.

[2] Mandeep R. et al. Mehra. The 2016 international society for heart lung transplantation listing criteria for heart transplantation: A 10-year update. *The Journal of Heart and Lung Transplantation*, 35(1):1–23, 2016.

[3] Marwan A. Simaan. Rotary heart assist devices. In *Handbook of Automation*, 2009.

[4] Marwan A. Simaan, Antonio Ferreira, Shaohi Chen, James F. Antaki, and David G. Galati. A dynamical state space representation and performance analysis of a feedback-controlled rotary left ventricular assist device. *IEEE TRANSACTIONS ON CONTROL SYSTEMS TECHNOLOGY*, 17(1), 2009.

[5] Eun jin Kim and Massimo Capoccia. Mechano-electric effect and a heart assist device in the synergistic model of cardiac function. *Mathematical biosciences adn engineerig*, 17(5):5212–5233, 2020.

[6] Brit Long, Jennifer Robertson, Alex Koyfman, and William Brady. Left ventricular assist devices and their complications: A review for emergency clinicians. *The American Journal of Emergency Medicine*, 37(8):1562 – 1570, 2019.

[7] Daniel Timms. A review of clinical ventricular assist devices. *Medical Engineering & Physics*, 33(9):1041 – 1047, 2011.

[8] Leslie W. Miller and Joseph G. Rogers. Evolution of Left Ventricular Assist Device Therapy for Advanced Heart Failure: A Review. *JAMA Cardiology*, 3(7):650–658, 2018.

[9] Bin Gao, Yizhou Kang, Qi Zhang, and Yu Chang. Biomechanical effects of the novel series lvad on the aortic valve. *Computer Methods and Programs in Biomedicine*, 197:105763, 2020.

[10] Massimo Capoccia. Development and characterization of the arterial windkessel and its role during left ventricular assit device assitance. *Artificial Organs*, 39:E138–E153, 2015.

[11] D. R. Warriner, A. G. Brown, S. Varma, P. J. Sheridan, P. Lawford, D. R. Hose, A. Al-Mohammad, and Y. Shi. Closing the loop: modelling of heart failure progression from health to end-stage using a meta-analysis of left ventricular pressure-volume loops. *PloS one*, 9(12):e114153, 2014.

[12] Abdul-Hakeem H AlOmari, Andrey V Savkin, Michael Stevens, David G Mason, Daniel L Timms, Robert F Salamonsen, and Nigel H Lovell. Developments in control systems for rotary left ventricular assist devices for heart failure patients: a review. *Physiological measurement*, 34(1):R1, 2012.

[13] C. Ozcan and A Deshmukh. Atrial arrhythmias in patients with left ventricular assist devices. *Current opinion in cardiology*, 35(3):276–281, 2020.

[14] Nico Westerhof, Jan-Willem Lankhaar, and Berend E. Westerhof. The arterial windkessel. *Medical & Biological Engineering & Computing*, 47(2):131–141, Feb 2009.

[15] Laura Marx, Matthias AF Gsell, Armin Rund, Federica Caforio, Anton J Prassl, Gabor Toth-Gayor, Titus Kuehne, Christoph M Augustin, and Gernot Plank. Personalization of electro-mechanical models of the pressure-overloaded left ventricle: fitting of windkessel-type afterload models. *Philosophical Transactions of the Royal Society A*, 378(2173):20190342, 2020.

[16] Urs Hackstein, Stefan Krickl, and Stefan Bernhard. Estimation of arma-model parameters to describe pathological conditions in cardiovascular system models. *Informatics in Medicine Unlocked*, page 100310, 2020.

[17] Nam Lyong Kang. Relationship between blood pressure and flow rate in arteries using a modified windkessel model. *arXiv preprint arXiv:2006.02590*, 2020.

[18] M. A. Bahloul and T. M. Laleg-Kirati. Assessment of fractional-order arterial windkessel as a model of aortic input impedance. *IEEE Open Journal of Engineering in Medicine and Biology*, 1:123–132, 2020.

[19] Duarte Valério and Jose da Costa. *An introduction to fractional control.* 01 2012.

[20] Clara Ionescu and James F. Kelly. Fractional calculus for respiratory mechanics: Power law impedance, viscoelasticity, and tissue heterogeneity. *Chaos, Solitons & Fractals*, 102:433 – 440, 2017.

[21] Miguel Angel Moreles and Rafael Lainez. Mathematical modelling of fractional order circuit elements and bioimpedance applications. *Communications in Nonlinear Science and Numerical Simulation*, 46:81 – 88, 2017.

[22] Richard L Magin. *Fractional calculus in bioengineering*, volume 2. Begell House Redding, 2006.

[23] Mihir Sen, John P. Hollkamp, Fabio Semperlotti, and Bill Goodwine. Implicit and fractional-derivative operators in infinite networks of integer-order components. *Chaos, Solitons & Fractals*, 114:186–192, 2018.

[24] A.-J. Guel-Cortez, M. Sen, and B. Goodwine. Closed form time response of an infinite tree of mechanical components described by an irrational transfer function. In *2019 American Control Conference (ACC)*, pages 5828–5833, July 2019.

[25] Adrián Josué Guel-Cortez, César-Fernando Méndez-Barrios, Emilio Jorge González-Galván, Gilberto Mejía-Rodríguez, and Liliana Félix. Geometrical design of fractional pdμ controllers for linear time-invariant fractional-order systems with time delay. *Proceedings of the Institution of Mechanical Engineers, Part I: Journal of Systems and Control Engineering*, 233(7):815–829, 2019.

[26] E. Kim and Massimo Capoccia. Synergistic modelling of cardiac function with a heart assist device. *Physical Review E*, under review, 2019.

[27] Mohamed A. Bahloul and Taous-Meriem Laleg Kirati. Fractional-order modeling of the arterial compliance: An alternative surrogate measure of the arterial stiffness, 2020.

[28] Mourad S. Semary, Mohammed E. Fouda, Hany N. Hassan, and Ahmed G. Radwan. Realization of fractional-order capacitor based on passive symmetric network. *Journal of Advanced Research*, 18:147 – 159, 2019.

[29] Pu Yifei, Yuan Xiao, Liao Ke, Zhou Jiliu, Zhang Ni, Zeng Yi, and Pu Xiaoxian. Structuring analog fractance circuit for 1/2 order fractional calculus. In *2005 6th International Conference on ASIC*, volume 2, pages 1136–1139, Oct 2005.

[30] James F. Kelly and Robert J. MacGough. Fractal ladder model and power law wave equations. *The Journal of the Acoustical Society of america*, 126(4):2072–2081, 2009.

[31] Abdon Atangana. *Fractional operators with constant and variable order with application to geo-hydrology.* Academic Press, 2017.

[32] AK Shukla and JC Prajapati. On a generalization of mittag-leffler function and its properties. *Journal of mathematical analysis and applications*, 336(2):797–811, 2007.

[33] Jocelyn Sabatier, Mathieu Merveillaut, Rachit Malti, and Alain Oustaloup. How to impose physically coherent initial conditions to a fractional system. *Commun Nonlinear Sci Numer Simulat*, 15:1318–1326, 2010.

[34] Jocelyn Sabatier. Fractional-order derivatives defined by continuous kernels: Are they really too restrictive? *Fractal and Fractional*, 4(3), 2020.

[35] Roberto Garrappa. Numerical solution of fractional differential equations: A survey and a software tutorial. *Mathematics*, 6(16), 2018.

[36] F. Seemann, P. Arvidsson, D. Nordlund, S. Kopic, M. Carlsson, H. Arheden, and E. Heiberg. Noninvasive quantification of pressure-volume loops from brachial pressure and cardiovascular magnetic resonance. *Circulation. Cardiovascular imaging*, 12(1):e008493, 2019.

[37] Marcelo B Bastos, Daniel Burkhoff, Jiri Maly, Joost Daemen, Corstiaan A den Uil, Koen Ameloot, Mattie Lenzen, Felix Mahfoud, Felix Zijlstra, Jan J Schreuder, and Nicolas M Van Mieghem. Invasive left ventricle pressure–volume analysis: overview and practical clinical implications. *European Heart Journal*, 41(12):1286–1297, 08 2019.

[38] David E. Mohrman and Lios Jane Heller. *Cardiovascular Physiology.* Lange Medical Books/McGraw-Hill. New York, USA, 9 edition, 2018.

[39] H. N. Sabbah, D. T. Anbe, and P. D. Stein. Negative intraventricular diastolic pressure in patients with mitral stenosis: evidence of left ventricular diastolic suction. *The American journal of cardiology*, 45(3):562–566, 1980.